ACS OMEGA

Open Access

http://pubs.acs.org/journal/acsodf

Article

Development, Evaluation, and Molecular Dynamics Study of Ampicillin-Loaded Chitosan−Hyaluronic Acid Films as a Drug Delivery System

Sema Arısoy, Khair Bux,* Ralf Herwig, and Emine Şalva

Cite This: *ACS Omega* 2024, 9, 19805−19815

Read Online

ACCESS | Metrics & More | Article Recommendations

ABSTRACT: Periodontitis is an inflammatory periodontal disease defined by the progressive loss of tissues surrounding the tooth. Ampicillin is an antibiotic for managing and treating specific bacterial infections, including periodontitis. Periodontal pockets occur due to periodontal disease progression and act as a natural reservoir that is easily reachable for the insertion of a delivery system, and the amount of drug to be released has a major role in the efficiency of treatment of the disease. Polyelectrolyte complexes (PECs), particularly those based on chitosan and hyaluronic acid combinations, offer a promising avenue to overcome the challenges associated with drug delivery. These complexes are both biodegradable and biocompatible, making them an optimal choice for enabling targeted drug delivery. This study centers on developing and assessing the structure and dynamic attributes of a drug−PEC system encompassing ampicillin and chitosan−hyaluronic acid components, which represents a targeted drug delivery system to better alleviate the periodontitis. To achieve this goal, we conducted experiments including weight and drug content uniformity, swelling ındex, drug release %, FT-IR and SEM analyses, and atomistic molecular dynamics simulations on the drug PECs loaded with ampicillin with varying amounts of hyaluronic acid. All simulations and the experimental analysis suggested that increased HA amount resulted in an increase in drug release % and swelling index. The simulation outcomes provide insights into the nature of the drug and PEC interactions alongside transport properties such as drug diffusion coefficients. These coefficients offer valuable insights into the molecular behavior of ampicillin−PEC drug delivery systems, particularly in the context of their application in periodontitis treatment.

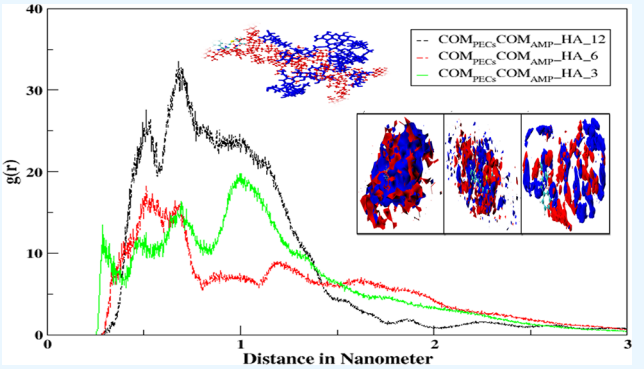

1. INTRODUCTION

The progressive loss of the tissues around the tooth is characterized by periodontitis, an inflammatory periodontal disease. More than 300 microorganism species have been found in the mouth in recent years, and its underlying cause is an unclear chain of microbial diseases.[1] In the first stage of treatment, mechanical debridement is utilized either alone or in conjunction with antimicrobial medications.[2] Treatment development is hindered by antibiotic- or antimicrobial-related side effects in cases of systemic periodontitis. One potential therapeutic option is to administer an antibiotic directly to the periodontal lesion using local drug delivery, which can achieve a high local medication concentration with few side effects. Given that the disease is limited to the periodontal cavity, the most effective method is to provide the medication locally through the pocket.[3]

Pockets formed by periodontal disease progress with time. The periodontal pocket is a convenient location to put a delivery system because it serves as a natural reservoir. A medicine can be released from its dosage form and diffused throughout the periodontal pocket, which also functions as a dissolving medium. Fewer side effects, more efficacy, and better patient compliance are all reasons why intrapocket drug delivery devices are desirable. The potential for maintaining effective medication concentrations in the pocket liquid for an extended length of time, leading to the intended therapeutic benefits, is the main attraction of using intrapocket drug carriers to treat periodontal illnesses.[2,4]

The effectiveness of periodontitis treatment is dependent on the release system's capacity to maintain the drug release rate.[5] To deposit and maintain the medication concentration in the

Received: October 15, 2023
Revised: April 8, 2024
Accepted: April 17, 2024
Published: April 29, 2024

periodontal pocket for an extended duration, local delivery techniques such as films, gels, and fibers are utilized.[2,3] One of the most common methods of intrapocket drug administration is the use of films composed of biodegradable or insoluble polymers. These films release the medication either through diffusion, drug and matrix dissolution, or matrix erosion.[2,6] These drug delivery systems use a polymer matrix that contains drugs that are disseminated or dissolved throughout.[2,3] The use of films has various benefits, such as less discomfort for the patient, appropriate sizing to fit the pockets, and convenience of insertion. Those that have an appropriate adhesiveness and are thinner than 400 μm are not easily removed by the patient's usual oral hygiene routine.[3]

Chitosan is a polysaccharide with a positive charge of the amino groups comprising glucosamine and N-acetyl-glucosamine copolymers. Chitosan is one of the best options to produce drug delivery systems aiming to be inserted in the periodontal pocket for periodontitis treatment due to its excellent film-forming ability along with antimicrobial, mucoadhesion, biodegradable, wound healing, and sustained drug release features.[7−9] Cross-linking is one of the most essential film-forming and drug release-controlling strategies for the chitosan-based drug delivery system.[5,8] Nontoxic polyanions are used to prepare chitosan films to form a polyelectrolyte complex.[8] Polyelectrolyte complexes (PECs) are complex molecular structures that are generated by a network of positively and negatively charged polymeric molecules, proteins, and nucleic acids in any ionizing solvent, such as water. Natural polymers with relatively facile ionic cross-linking, such as positively charged chitosan and anionic molecules like hyaluronic acid (HA), are often utilized to produce drug delivery systems.[5] HA is a linear glycosaminoglycan composed of replicating disaccharide units of N-acetyl-D glucosamine and D-glucuronic acid. Because of its exceptional biodegradability and biocompatibility, HA has potential uses in tissue engineering and wound healing. Despite the use of other toxic chemicals to achieve cross-linked structures with chitosan, HA emerges as a nontoxic alternative.[9,10] Given the tissue loss that occurs during the progression of periodontitis, HA has the potential to aid in the tissue regeneration process.[1,10] Miranda and Malmonge[11] developed a chitosan-HA cross-linked hydrogel scaffold for periodontal tissue regeneration. They discovered CD44-HA interactions in the control of matrix metalloproteinases, supporting the concept that HA-based scaffolds are adequate biomaterials for periodontal regeneration. Chitosan's clinical efficacy in treating chronic periodontitis was examined by Akıncıbay et al.[12] Due to its antibacterial characteristics, chitosan, individually and in combination with metronidazole, has been demonstrated to be beneficial in treating periodontitis. Khajuria and Patil[13] developed a chitosan-metformin dental film by solvent casting method to treat periodontitis and alveolar bone loss in a rat model. Chitosan-metformin dental film demonstrated antibacterial properties and effectively reduced alveolar bone damage in this experimental periodontitis model.

Ampicillin treats bacterial infections such as chest infections (including pneumonia) and dental abscesses. However, oral amoxicillin is generally used as the first line of treatment in nonallergic individuals for periodontitis therapy, whereas IV or IM amoxicillin is often used for those who cannot take medicines orally.[14] Ampicillin is used as an alternative to amoxicillin due to its comparable antibacterial efficacy. Also, ampicillin is more soluble than amoxicillin, making it an option for local administration in periodontal pockets.[15]

In light of this literature knowledge, it was planned to design a chitosan-HA-based, ampicillin-loaded film to apply to the periodontal pocket for periodontitis treatment. Chitosan was chosen for its antibacterial efficiency along with ampicillin to treat periodontitis, a bacteria-induced disease, and for mucoadhesion properties to be fixed in the periodontal pocket.[1−4,6−8] Chitosan would also regenerate tissue surrounding the tooth due to its wound healing capacity.[1−4,6−8] HA was chosen for wound healing abilities and as a cross-linker to obtain PECs for sustained drug release to hinder frequent dosing.[9,10] As a result, chitosan and hyaluronic acid were formulated, and characterization studies on films were performed to develop ampicillin-loaded PECs as a unique combination for periodontitis treatment.

Molecular dynamics (MD) simulations are powerful computational techniques used to investigate the behavior of atoms and molecules over time, and MD simulation could be used as a supporting tool to understand the drug loading and controlled release mechanisms of drug delivery systems. They are precious in studying complex systems, such as intrapocket polyelectrolytic drug delivery systems, where traditional experimental approaches might be challenging or costly. Overall, MD simulations offer a complementary approach to experimental methods in studying interpocket PEC drug delivery systems, enabling researchers to gain atomistic-level insights and accelerate the drug discovery and development process.[16] However, it is essential to remember that MD simulations are computationally intensive and require careful validation with experimental data for accurate predictions.

Because previous studies lack detailed insights into molecular mechanism drug encapsulation in chitosan-based drug delivery systems, in this study, a drug delivery system was designed to obtain a local treatment alternative and to sustain drug release for the whole treatment period of periodontitis. Ampicillin was used as a model drug to develop a new film by cross-linking with chitosan and HA to form a PEC-based system. The binding of ampicillin to and release of ampicillin from PECs was investigated at atomic levels by MD simulations along with the formulation characterization studies. This comprehensive approach allowed us to investigate the behavior and interactions of ampicillin with PECs formed by chitosans and HA in varying ratios, facilitating a deeper understanding of their properties and potential applications in drug delivery systems.

2. MATERIALS AND METHODS

2.1. Material. Medium molecular weight chitosan was purchased from Sigma. HA was obtained from Rang Pang. Propylene glycol was purchased from Merck. Ampicillin was purchased from Serva Pharmaceuticals.

2.2. Methods. *2.2.1. Preparation of PECs.* HA, propylene glycol, and ampicillin solutions is mixed in the tube and then dropwise added to chitosan solution with a thin needle. Ampicillin at 1.0% of the[17] and propylene glycol (5%, v/v) as a plasticizer was used in the formulation.[5] The solution was poured into 10 cm radius plates and then dried overnight in a 37 °C incubator. Dry film formulations (details given in Table 1) were cut in the dimension of 1 × 1 cm.

2.2.2. Characterization of PECs. 2.2.2.1. Weight Uniformity. The weight uniformity test was performed by weighing three pieces of film with a diameter of 1 cm. The

https://doi.org/10.1021/acsomega.3c08076
ACS Omega 2024, 9, 19805−19815

Table 1. Formulation Variables

formulation	chitosan, %	hyaluronic acid, %	drug content
I1	2	12	1 mg/mL ampicillin
I2	2	12	water
I3	2	6	1 mg/mL ampicillin
I4	2	6	water
I5	2	3	1 mg/mL ampicillin
I6	2	3	water

weights of the films were calculated and expressed as the average weight SD.

2.2.2.2. Drug Content. In a glass beaker, the film was dissolved with 2 mL of 1% acetic acid phosphate buffer pH 7.4 and sonicated for 5 min. It was then filtered via a 0.5 m membrane filter, and the drug content was determined by using UV.

2.2.2.3. Swelling Index. A phosphate buffer solution pH 7.4 was used to test the swelling of the films. This procedure necessitated using a Petri dish and a digital analytic scale. Dry film was weighed and 1 mL of phosphate buffer pH 7.4 was poured onto the dry film, and the excess water was absorbed with filter paper. The weight of the film increases at constant predetermined time intervals until there is no more weight rise. These factors can then be used to calculate the swelling index:

$$\text{Swelling index} = (w_t - w_0)/w_0)$$

w_t, weight of film at time interval t (final weight); w_0, weight of film at time 0 (initial weight).

2.2.2.4. In Vitro Drug Release. 50 mL portion of buffer pH 7.4 was employed as the dissolving media. The temperature was kept constant at 37 ± 0.5 °C, and the rotation speed was adjusted to 50 rpm. A 1 mL sample was withdrawn and replaced with 1 mL buffer at predetermined intervals. The UV technique was used to determine the concentration of dissolved drug samples collected at the time points.

2.2.2.5. IR Spectrum Study. Fourier transform infrared (FT-IR) studies were carried out to analyze the possible drug−excipient interaction. The FT-IR spectra of pure drug, film former, and films were recorded using an FT-IR spectrometer (PerkinElmer-UATR two) over a scan range from 4000 to 400 cm^{-1}. The FT-IR spectra of the ampicillin (pure drug), film former (Chitosan, HA), and oral films were compared to determine drug-excipient interaction.

2.2.2.6. Film Morphology and Thickness Using a Scanning Electron Microscope. Oral films were characterized by scanning electron microscopy (SEM)(Leo Evo 40-SEM). The film was placed vertically by sitting in a sticky paste. Surface morphology and thickness were obtained during the test.

2.2.3. MD Simulations. Before carrying out MD simulations, quantum chemical calculations were separately performed to optimize the structure of chitosan at a 75% level of deacetylation according to the product specifications used in experimental studies. In addition, as shown in Figure 5. modeled structures of HA, chitosan and ampicillin were optimized at the same level of theory. Simulations were performed following the published literature by Shen and Li.[18]

The AMBER[19] suite's LEaP module generated the structural and topological representations of chitosan containing 10 units of HA, and ampicillin. Subsequently, we created the initial structures of 10 unit chitosans by substituting 25% of the glucose unit's −OH groups bonded with C2 with −NHCOCH3 and 75% through deacetylation to −NH2, as illustrated in Figure 5. The optimization of the geometries of chitosan units, HA, ampicillin, and PECs within various groups was performed using the HF/6-31G+ method via Gaussian03 software. Following this, the force field parameters were obtained, encompassing atom charges and bonded/nonbonded parameters. These parameters for chitosan units with various functional groups were derived from the OPLSAA force field. The parameters for bond lengths, angles, and dihedral angles between distinct chitosan units were extracted from references. Additionally, the partial charges were determined by employing the restrained electrostatic potential (RESP) method, calculating chitosan units featuring different functional groups at the HF/6-31G+ level using Gaussian 03.

2.2.3.1. Simulation Protocol. All simulations were conducted utilizing the GROMACS 5.0.7 package.[20] In each system, a specific number of chitosans and polynucleotide chains, as indicated in Table 2, were immersed within a box

Table 2. Optimized Number of Chitosan−HA-Based Systems Loaded with Ampicillin

number of chitosan	number of HA	ampicillin	type of system
2	12	1	PECs_large
2	6	1	PECs_medium
2	3	1	PECs_small

filled with TIP3P[21] water molecules, accomplished with packmol software. Counterions (Na+ or Cl−) were introduced to neutralize the systems. Periodic boundary conditions were applied, and a time step of 2 fs was employed. The van der Waals (vdW) interactions were truncated at 1.2 nm, while the LINCS algorithm[22] was employed to restrain bond lengths. Electrostatic interactions were computed utilizing the particle mesh Ewald (PME) method[23] with a 1.2 nm cutoff. The Lennard-Jones (LJ) potential for cross-interactions between chitosan and polynucleotides was calculated according to the Lorentz−Berthelot rule.[24] Temperature was controlled at 300 K via velocity rescaling,[25] and pressure was regulated at 1 bar using the Berendsen method[26] with an isothermal compressibility of 4.5×10^{-5} bar^{-1}. In each system, a 50,000-step energy minimization was initially carried out using the steepest descent method.[27] Subsequently, a 10,000 ps pre-equilibration was conducted under an NVT ensemble.

Finally, a **200 ns MD** simulation was performed in the NPT ensemble. For visualization and analysis of the simulation results, we utilized the visual MD (VMD) graphics software.[28]

2.2.3.2. Molecular Mechanics/Poisson−Boltzmann Surface Area Analysis. Molecular mechanics/Poisson−Boltzmann surface area (MM-PBSA) analysis was performed according to published literature before.[29] The g_mmpbsa tool plays a crucial role in determining the binding free energy of polyamine-polyanions such as chitosan-HA complexes by analyzing MD trajectories. In inhibitor screening, binding free energy calculations using the MM/PBSA method during postsimulation analysis have gained widespread use. Notably, this approach has displayed reasonable agreement with the experimental findings. Recognizing the significance of system entropy and considering that the g_mmpbsa method does not directly compute the entropy component, we estimated it by employing the Schlitter formula. To facilitate this estimation, covariance matrices for the complexes were generated from the

https://doi.org/10.1021/acsomega.3c08076
ACS Omega 2024, 9, 19805−19815

Table 3. Weight and Drug Content Uniformity of Formulations (n = 3)

	I1	I2	I3	I4	I5	I6
weight	6.3 ± 0.1	4.73 ± 0.25	5.8 ± 0.2	4.1 ± 0.1	5.2 ± 0.2	4.3 ± 0.1
drug content (mg)	0.294 ± 0.197		0.312 ± 0.211		0.13 ± 0.002	

last 60 ns of the MD simulations using gmx covar. Subsequently, at a temperature of 300 K, entropy values were computed using the gmx anaeig tool. The entropy was determined using the following equation:

$$\Delta S = S_{\text{complex}}(S_{\text{protein}+}S_{\text{ligand}})$$

The postsimulation binding free energy (DG) was calculated using the following equation:

$$\Delta G = \Delta G_{\text{electrostatic}} + \Delta G_{\text{vdw}} + \Delta G_{\text{polar}} + \Delta G_{\text{non-polar}} - T\Delta S$$

In this investigation, the nonpolar solvation energy (DG nonpolar) corresponds to the SASA energy (DGSASA) due to its reliance on the SASA model to compute nonpolar solvation energy. Using the g_mmpbsa tool, we analyzed the total binding free energy to decompose into the individual residue contributions. Enabled the identification of residues that significantly influenced the binding process.

3. RESULTS AND DISCUSSION

3.1. Formulation Development and Characterizations. Films are polymer-based matrix delivery methods in which pharmaceuticals are dispersed throughout the polymer and released via drug diffusion and/or matrix dissolution or erosion. This dosage form has various physical features that make it ideal for intrapocket usage.[4] Numerous biopolymers have previously been explored for the production of oral mucoadhesive films, not only because of their exciting biocompatibility and biodegradability but also because of their appealing molecular structures with active groups, which could potentially be used to physically or chemically interact with the mucin present in the oral mucus, allowing desirable mucoadhesive properties and bringing significant advantages to absorption of drugs.[30] In this study, chitosan and HA structured PECs were loaded with ampicillin to treat periodontitis as a promising drug delivery system with mucoadhesive properties. Using bioadhesive films leads to a prolonged stay in the oral cavity, adequate medication penetration, excellent efficacy, and acceptance. Various approaches to chitosan, a bioadhesive polymer, have been proposed in dentistry and oral medicine because of its beneficial features such as biocompatibility and biodegradability.[31] HA was used as a cross-linking agent in the formulation. HA has a negative charge, while chitosan has a positive one, leading to a cross-linked PEC formulation when appropriately mixed. In this study, different amounts of HA were added to the formulation to obtain desirable drug release. HA is a natural polysaccharide comprised repeated D-glucuronic acid and N-acetyl glucosamine disaccharide units connected by −1,4 and −1,3 glycosidic linkages. Because of its unique bioactivity, biocompatibility, and nontoxicity, HA has been employed successfully in pharmaceuticals, cosmetics, and functional foods.[32] An earlier study indicated a promising application of chlorhexidine gluconate at a low concentration (0.1%) incorporated into chitosan gel for candidiasis in the oral cavity.[31,33]

3.1.1. Determination of Oral Film Characteristic. Local drug delivery has unique advantages in lowering applied doses compared with oral therapy. So, in this study, a lower concentration of ampicillin than an oral dose was used in the formulation. The plasticizer is a vital ingredient in the oral film formulation. It helps to improve the flexibility of the strip and reduces the brittleness of the strip. Typically, the plasticizers are used in a concentration of 0−20% w/w of dry polymer weight.[34] In this study, 5% propylene glycol was used for this purpose. All prepared formulas exhibited an excellent uniformity of weight with low deviation among manufacturing replications (Table 3). The higher concentration of HA resulted in an increase in the weight of the films per cm^2, as shown in the increase in weight from I5 to I1. Drug content differences was discussed according to MD studies in Section 3.2.1.

The swelling property is a critical parameter in the formulation of films. The swelling index is a metric that describes the swelling properties of film when it comes into contact with an aqueous media.[35] Chitosan films were generated using the casting method, and Figure 1 illustrates

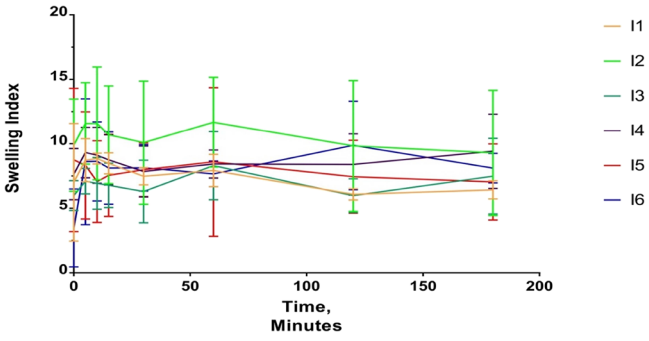

Figure 1. Swelling index of formulations vs time (n = 3).

the quality of the produced chitosan films. According to Figure 1, the swelling index of the films increased substantially at first, and the chitosan films appeared to be entirely swelled and hydrated after 15 min. This was owing to the porous structure and hydrophilicity of the chitosan film, which indicated a significant hydration of chitosan, facilitating its rapid mucoadhesion in drug administration.[36] As shown in Figure 1, the swelling index versus time was similar between all formulations. I1, I3, and I5 formulations loaded with ampicillin showed a lower swelling capacity. The high values of the swelling index indicate that water molecules can easily penetrate the polymer.[35] This decrease could be because the pores were filled with drugs and the water intake was hindered. A discussion of these results in the light of MD studies is presented in Section 3.2.3.

At the 336th h, the I1 coded oral film released 87% of loaded ampicillin (Figure 2) which suggests that ampicillin release increased with the HA concentration. Changing the HA concentration (6% vs 3%) had no influence on the released percent from I3 or I5. After 72 h, the release of ampicillin from films hit a plateau. In 336 h, a total of 33 and 32% of ampicillin

https://doi.org/10.1021/acsomega.3c08076
ACS Omega 2024, 9, 19805−19815

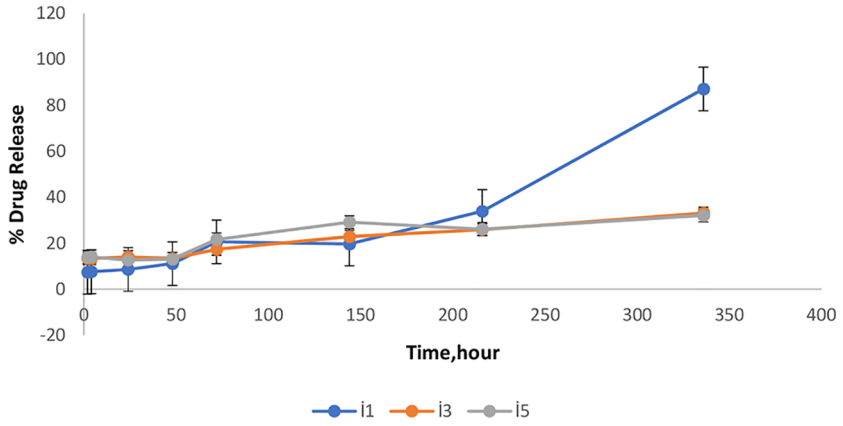

Figure 2. In vitro relase of ampicillin from oral films (n = 3).

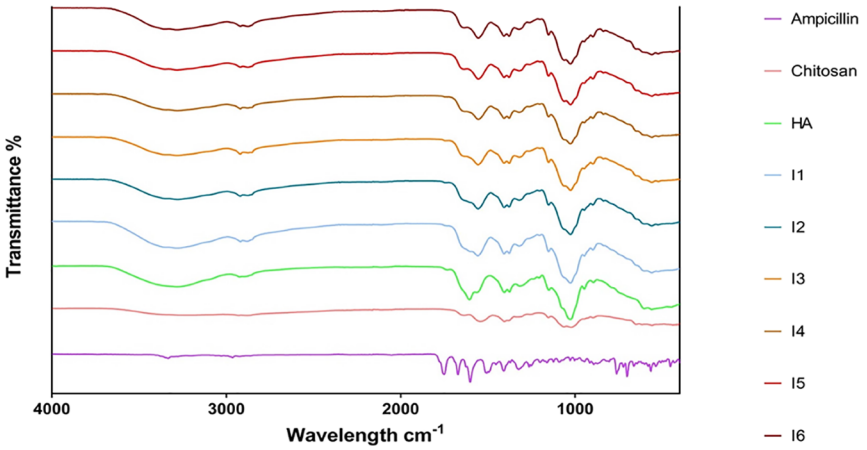

Figure 3. FT-IR images of formulations chitosan, HA, and ampicillin.

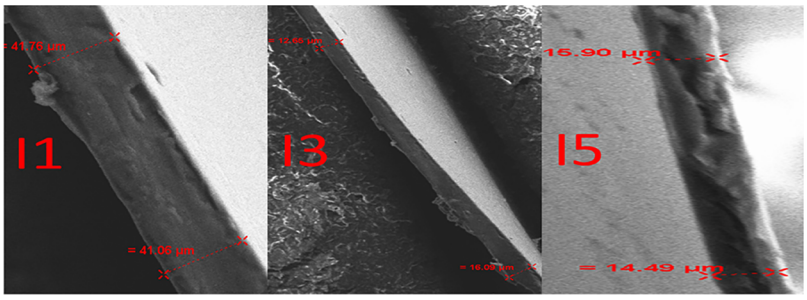

Figure 4. SEM images of ampicillin-loaded oral films.

were released from the films containing 6 and 3% HA, respectively, whereas 87% was released from the 12% HA cross-linked film. There was no lag time in the release of the films. Release study results are discussed at the atomic level in Section 3.2.2.

The two peaks at about 1600 cm^{-1} corresponding to the overlapping of the amide I and II peaks and the N−H bending vibration of the amine groups present in the deacetylated units are visible in the chitosan spectrum. The HA spectra showed multiple strongly overlapped peaks in the carbonyl stretching vibration band between 1500 and 1800 cm^{-1}. The antisymmetrical stretching vibration in the carbonyl group of the carboxylate was assigned the most significant peak in this region (1534.0 cm^{-1}) (−COO−).[37] The presence of ionic interactions is confirmed by the FT-IR spectra of chitosan−HA PECs from 1200 to 1700 cm^{-1} (Figure 3). The positively charged amino group of chitosan (as shown by the NH3+ bending vibrations (1550 cm^{-1}) interacts with the negatively charged −COOH of hyaluronic acid (as observed by the 1610 cm^{-1}) PEC creation and cross-linking also resulted in lower absorption for the O−H and N−H stretching vibration peaks.[38] Ampicillin did not affect the interaction of chitosan and HA since no other distinctive peaks changed significantly.[37]

During the SEM studies, the thickness was also measured. As shown in Figure 4, ampicillin-loaded films coded I1, I3, and I5 showed different thickness values that may be due to HA amount in the films, which are acceptable thickness as an oral film. If the film's thickness does not exceed 400 μm and it has appropriate adhesiveness, it will remain submerged without

https://doi.org/10.1021/acsomega.3c08076
ACS Omega 2024, 9, 19805−19815

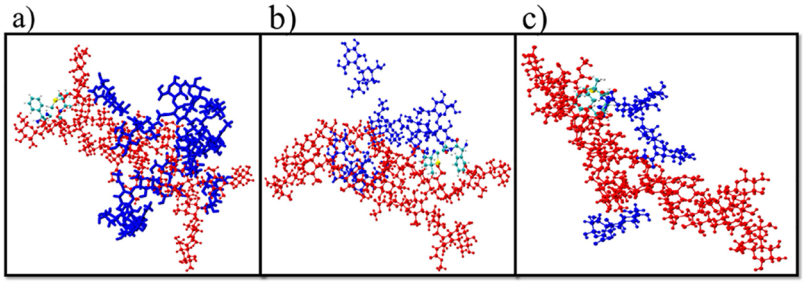

Figure 5. Modeled structures of formulations at different HA levels: (a) PECs_small, (b) PECs_medium, and (c) PECs_large (blue: chitosan, red: HA, cyan: ampicillin).

interfering with the patient's dental hygiene routines.[4] As shown in Figure 4 the higher concentration of the film former resulted in increased thickness, which is implicated in an increase in the weight of the formulated films. Thickness homogeneity is an essential physical feature in oral film evaluation because it significantly impacts the precision of film dosage distribution.[35]

3.2. MD Simulations. MD studies were carried out to better interpret the experimental studies' results by understanding the prepared system's molecular interactions. The MD study findings were analyzed by combining them with the experimental results.[16]

3.2.1. Determination of Ampicillin-Binding Effect. The fundamental interactions were characterized by the computation of radial distribution functions (RDFs) between the drug and PECs at different levels of HA combinations, as shown in Figure 5.

The RDF generally relied on the $g(r)$ pair distribution function or pair correlation function that signifies the variation in density of selected molecules as a function of distance from reference molecules in the system. As represented in the following equation representing the evaluation of RDF (in the case of a liquid system)[39]:

$$g(r) = \frac{\langle \rho(r) \rangle}{\rho}$$

where $\rho(r)$ represents the average locale number density and bulk density (ρ) at a distance r.

Therefore, to figure out the effect of variation in HA amount on the drug-binding effect capacity of PECs, RDFs were computed between the center of mass of PECs for the three systems, as shown in Table 4. During the RDFs computations for three systems, the first shoulder and maxima peak were considered to understand how closely ampicillin interacts with PECs and spends most of its time at maximum occupancy. As shown as a black line in Figure 6, the RDFs between the center of mass of PECs and the ampicillin in the case for HA_12 exhibited distinct peaks at ~0.35 nm and a maximum, shoulder

Table 4. Free Energy of Binding of PECs (Chitosan and HA) with Ampicillin

	free energy of binding	HA_12	HA_6	HA_3
1	Van der Waals ΔG_{vdw}	−19.21	−21.02	−12.99
2	Van der Waals ΔG_{EEL}	−0.02	−5.02	−22.56
3	surface ΔG_{SURF}	−2.75	−3.41	−3.67
4	solvation ΔG_{SOLV}	5.27	−26.03	−35.54
5	gaseous ΔG_{GAS}	−19.38	10.93	13.84
6	total binding energy $\Delta G_{binding}$	−14.11	−15.11	−21.70

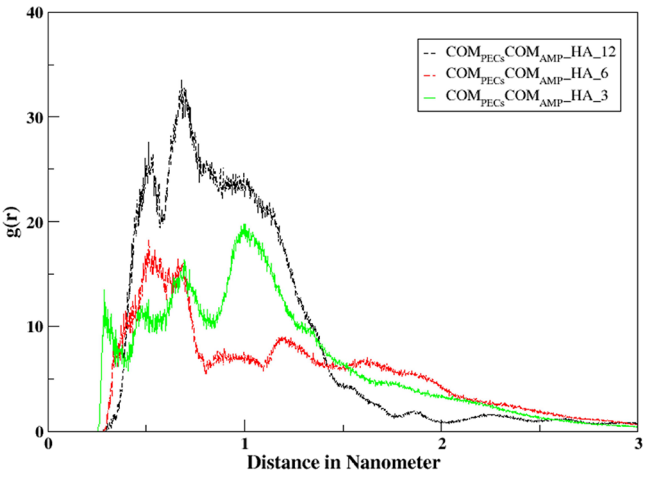

Figure 6. Radius of gyration $g(r)$ profiles of different systems with respect to the center of mass (COM) of ampicillin.

peak at 0.5 nm, therefore indicating the drug spends most of the time at the longer distance of 0.5 nm due to the hydrophobic effect as the number of HA increases. In the case of HA_6, no such strong shoulder peak was observed for RDFs, as depicted in red in Figure 6, between the center of mass of PECs and the ampicillin. However, a maximum peak was observed at 0.302 nm, showing the decreasing hydrophobic effect as the number of HA decreases. However, no appearance of sharp shoulder peaks indicates that the drug is relatively more dynamic, which was reasoned to be a balancing effect of hydrophobic and hydrophilic interactions.

Similarly, in the case of the H_6 system, a significant and robust shoulder peak at 0.27 nm was observed, followed by another peak at 0.30, and thus, hydrophilic forces were deduced to be dominating in this case of a minimal number of HA. Hence, the drug was observed to spend most of the time within this average domain of 0.35 nm.

Since chitosan and HA relatively contain hydrophobic moieties, RDF estimations showed the drug interacted with PECs at longer distances in the case of HA_12 due to having a larger number of HA due to the increasing hydrophobic effect.

RDFs represent the distance-based interactions and are limited in the angular representation that was of prime importance to acquire a complete picture of interactions and dynamics of the drug around the PECs since all the PECs systems were evaluated on the basis of relative anisotropic interaction potential in which local arrangements of interacting molecules were also assumed to be asymmetrical with respect to the reference molecule.

https://doi.org/10.1021/acsomega.3c08076
ACS Omega 2024, 9, 19805−19815

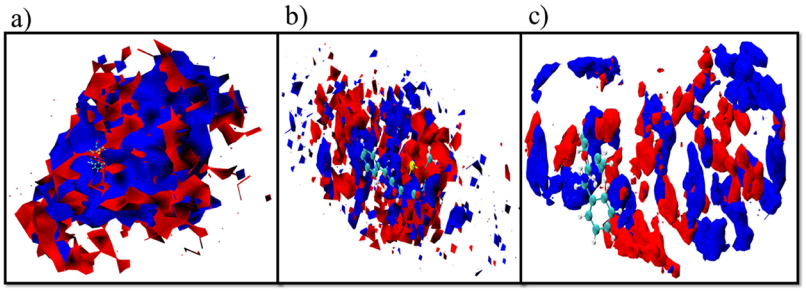

Figure 7. Spatial distribution function of PECs at different HA levels, (a) PECs_small, (b) PECs_medium, and (c) PECs_large (blue: chitosan, red: HA, cyan: ampicillin).

As deduced from the RDF estimations, the increasing number of HA was the reason for the increasing number of hydrophobic effect and thus affecting the drug interactions with PECs, as ampicillin was found to be interacting relatively at a longer distance under dynamical nature in the case of H_12. Spatial distribution functions (SDFs) were applied to obtain complete information on the spatial arrangements of PECs atomic particles (nitrogen and oxygen atoms of chitosan and HA) with reference to a predefined set of center of mass of ampicillin.

SDFs consider not only the radial spherical coordinates but also the angular spherical coordinates, thus characterizing the local 3D packing of PECs. Figure 7 depicts the SDFs for PECs comparatively around the center of mass of ampicillin. SDF analysis showed varying densities of PECs distribution in different regions of space as a function of different domains, as in the case of the HA_12 drug (Figure 7), the drug was found to be more distant to PECs that were found to experience more hydrophobic push out, and thus, ampicillin was found to be observed these forces and distant to PECs density. Whereas, in case, the HA_6 drug was observed relatively at a closer distance, and hydrophobic push out of the PECs seemed diminished, and thus, the drug got comparatively closer. Similarly, SDF maps showed the drug getting even closer to PECs density at a minimum number of HA in the case of HA_3 systems.

Following the RDF and SDF analyses, the drug-binding capacity of the PECs at variable amounts of HA was further evaluated by estimating the number of H bonds for the three systems. For the hydrogen-bonding analysis, the standard distance and angle between the donor and acceptor atoms were set around 3.0 Å and 135°, respectively. Figure 8 shows the number of hydrogen bonds between ampicillin and the PECs. Chitosan and HA, which complemented the RDFs and SDF observations like the number of hydrogen bonds between the ampicillin and PECs were observed comparatively lower in the case of HA_12 than in HA_6 and HA_3 systems. Moreover, based on the H-bonding analysis, it was deduced that ampicillin was experiencing a more hydrophobic effect and less hydrogen-bonding hydrophilic interactions with increased HA.

In order to find more detailed data on the interactions between PECs and ampicillin at variable numbers of HA, binding free energy was calculated by the MM/PBSA method.[29] The detailed analysis of binding free energies and energy components of the complexes is listed in Table 4. The results showed the drug to have stronger binding with larger negative free energy of binding about −21.21 kJ/mol in the case of HA_3 containing a lower number of HA. In contrast,

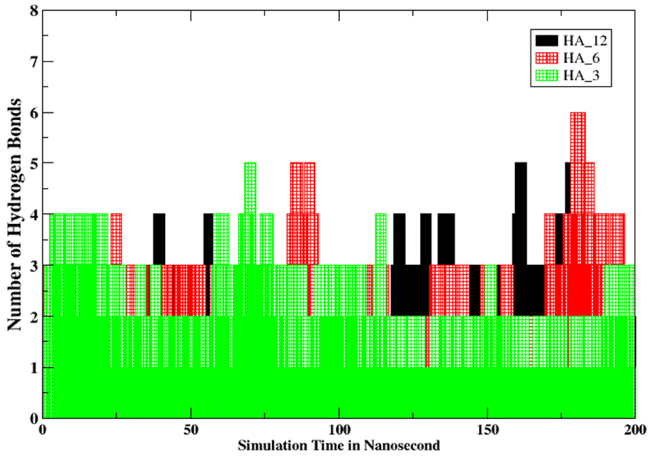

Figure 8. Number of intermolecular H bonds between three different systems and ampicillin as a function of time.

the drug was observed to be weakly bound in HA_6 and HA_12 with the free energy of binding about −15.21 and −14.12 kJ/mol, respectively. In order to obtain a better understanding of which interaction term had the most significant impact on the calculated binding energy, four energy components, including van der Waals (DEvdw), electrostatic (DEele), polar solvation energy (DGpol), and nonpolar interactions (DGnonpol) were computed. The results are tabulated in Table 4 and Figure 9, showing that DEvdw and DEele were remarkably contributing factors in the ampicillin and PECs binding at variable amounts of HA. In particular, it was apparent that van der Waals interactions, the important noncovalent interactions constructed by these compounds, highly influenced the binding of ampicillin to the PECs as shown in Figure 9 and Table 4, and H_12 was observed to have higher (DEvdw) energy than H_6 and HA_3. However, HA_3 was observed to have higher (DEele) components, showing that at lower HA levels, the drug experienced larger electrostatic interactions as deduced in hydrogen-bonding analysis.

This finding supports the experimental finding of this study, as shown in Table 3. Even though the ampicillin per cm^2 should be the same at different formulations, I5 (3% HA) was found to have a lower drug content than I1 (12% HA). It might be attributed to due to the decreased amount of HA ampicillin had stronger binding to PEC with larger negative free energy of binding about −21.21 kJ/mol. Even during the sonication process, ampicillin continued to interact with polymers, which hinders to be detected in UV.[40] However, the drug content was found higher for I3 (6% HA) than I1

https://doi.org/10.1021/acsomega.3c08076
ACS Omega 2024, 9, 19805−19815

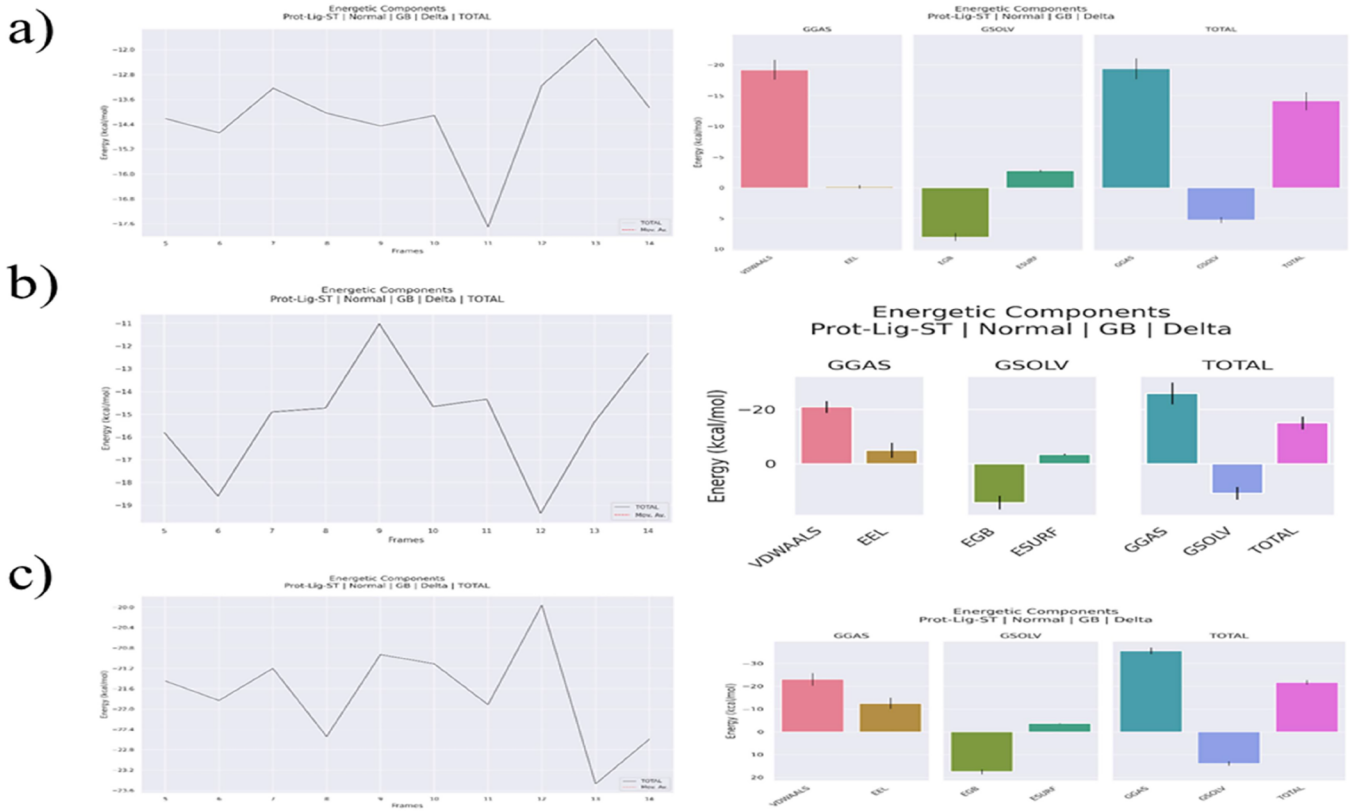

Figure 9. Depiction of binding affinity of ampicillin to PECs by obtained total binding free energies (kJ/mol) and involved compounds with bar plots for (a) H_12, (b) HA_6, and (c) HA_3 systems.

(12% HA). This might be attributed to the phenomenon that competition between solvent accessibility to the system and the binding energy of ampicillin to the system affected the results.[41]

3.2.2. Determination of Ampicillin Release from PECs. Ampicillin demonstrated a binding affinity for the PECs when introduced into an aqueous solution, as depicted in Figure 7 following the simulation. This configuration served as the model for drug delivery, necessitating an assessment of the sustained release mechanism. To ascertain the diffusion rate of the ampicillin, it was imperative to compute the diffusion coefficient within the simulation setup. Notably, different diffusive behaviors have been documented for molecules. Ultrafast and ballistic diffusion occurs when β equals 1, signifying normal diffusion where molecules emerge after collisions. On the other hand, when β is less than 1, it indicates a supercollision phenomenon akin to a cage escape behavior. The drug's diffusion was quantified by assessing the diffusion coefficient through mean square displacement (MSD), with both properties being interconnected through Einstein's relation.[39]

$$D = \frac{1}{2d}\lim_{t\to\infty}\frac{\mathrm{d}}{t}[r(t) - r(0)]^2$$

In this context, "d" represents the dimensions in the given system, with "d" equal to 3. "t" corresponds to the time range of the simulation, and "D" stands for the diffusion coefficient, measured in cm^2/s. On the other hand, "MSD" quantifies the extent of system position deviation within the systems concerning a reference point throughout the time. To attain a more precise characterization of the drug's diffusive properties, we determined the β value using the following equation. This "β" value indicates various diffusive behaviors, as previously mentioned.[39]

$$\beta(t) = \frac{d\log(\Delta r^2(t))}{d\log(t)}$$

The primary characteristic of a target-based drug delivery system is its ability to achieve sustained drug release, a property intricately linked to the change in diffusion with respect to the given time. Consequently, we assessed the diffusion of the ampicillin molecule by examining the diffusion coefficient, which was determined through the MSD data obtained for the drug in various systems, as illustrated in Figure 10 and summarized in Table 5. The system HA_12 with a higher number of HA yielded the drug diffusion coefficient 0.076 (±0.0830), which was higher than that of the system HA_6, where the drug was observed to have a diffusion coefficient of about 0.0323 (±0.0362) s. Whereas, in the case of HA_3 with significantly less HA in which the drug was observed to have stronger binding, showed the least diffusion coefficient of the drug, 0.0107 (±0.0207), thus showing the increase in HA to the system enhances the diffusion rate of the drug and decreases the tight binding of the drug with PECs.

This result, which was based on how the drug diffuse out through the modeled drug delivery systems, fit well with our experimental results that increased HA amount causes the higher release of drug from chitosan-based drug delivery systems.[18] As shown in Figure 2, I1(12% HA) coded formulation with the highest HA amount reached the highest drug release as 87%, while I5 (3% HA) and I3 (6% HA) released 32 and 33% of ampicillin in 336 h, respectively. In the

https://doi.org/10.1021/acsomega.3c08076
ACS Omega 2024, 9, 19805−19815

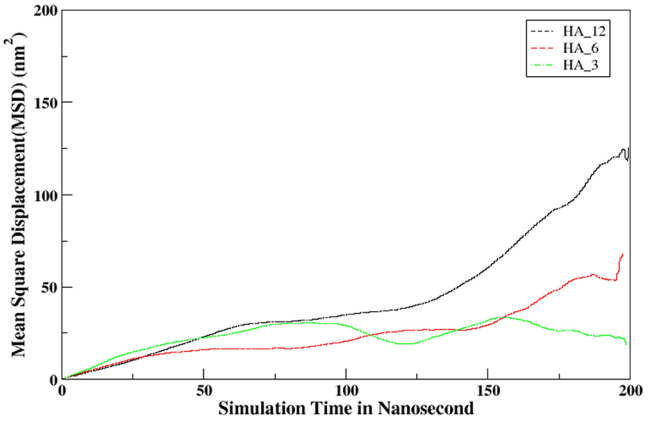

Figure 10. MSD plots for different systems vs simulation time (ns).

Table 5. MSD and Diffusion Coefficients of Different Systems

mean square displacement (MSD) $(nm)^2$	diffusion coefficients 10×−5 cm^2/s	system
198.884	0.076 (±0.0830)	HA_12
188.482	0.0323 (±0.0362) s	HA_6
175.295	0.0107 (±0.0207)	HA_3

case of systems HA_3, HA_6, and HA_3, the monomeric units presented differences in the drug diffusion coefficients, as evidenced by the MSD plots; however, they also showed significant fluctuations, which may be attributable to the drug's relative interaction with the PEC. This suggested that the addition of hydrophobic moieties to the HA increased the dynamic nature of the drug-PEC interactions. For this reason, it is recommended that such medication delivery devices have about the median quantity of HA.[40] The drug PECs interaction at a lower number of HA was reflected to have the lower retention time and more dynamics of the drug; thus, retention time significantly increased with the decrease in the number of HA. Similarly, the trend was the same observed in the case of our experimental studies, correlating the interaction energy calculations and RDFs.

3.2.3. Characterization of PEC Clusters (Size, Shape, and Compactness). PECs were further characterized by the assessment of their shape and size compactness by means of the radius of gyration. In Figure 11, the time evolution of *Rg* within the PECs-based simulation systems is illustrated, revealing significant fluctuations, particularly in HA_12. These fluctuations can be attributed to hydrophobic interactions. Conversely, the reduction in the quantity of HA in the system, specifically HA_6 and HA_3, contributed to the increased rigidity. By analyzing the *Rg* plot, we computed average values for all systems, noting that the *Rg* of the HA_12 system was notably larger at 26.4348 compared to the HA_6 and HA_3 systems, which had relatively lower amounts of hyaluronic acid (as depicted in Figure 12).

The PEC systems are situated within an aqueous solution, implying a hydrodynamic environment. Furthermore, to evaluate solvent and water molecules in orchestration of hydrodynamics of PECs and its influence on drug binding, solvent accessibility was estimated by means of solvent accessible surface area (SASA), as shown in Figure 12. SASA measures the exposure of PECs atoms to the solvent (water). We obtained respective SASA values in all systems, revealing

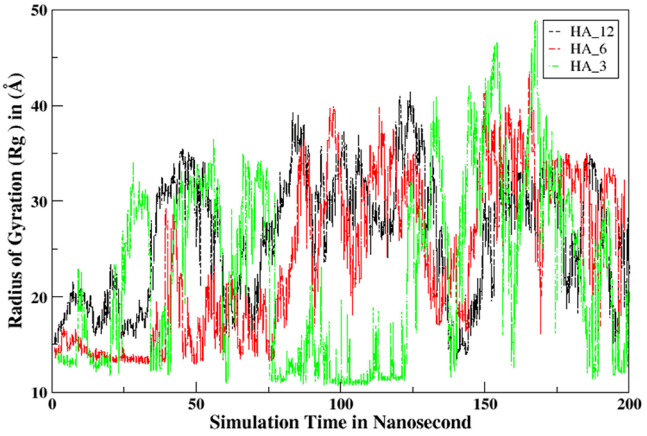

Figure 11. Time evolution of *Rg* within the different PEC-based simulation systems.

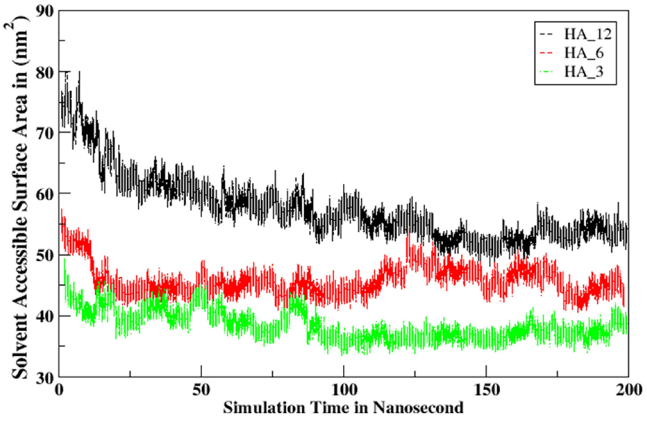

Figure 12. Time evolution of SASA within the different PEC-based simulation systems.

that PEC atoms in the HA_12 system were more exposed to the solvent, as indicated by the larger SASA value of 57.5273. In contrast, HA_6 and HA_3 systems exhibited comparatively lower SASA values of 45.7723 and 38.4362, respectively, signifying that these systems had PEC atoms that were less solvent-exposed, suggesting strong binding and protection from the solvent. As shown in Figure 1, PECs loaded with ampicillin (I1, I3, I5) showed lower swelling index versus time, unlike their unloaded equivalents (I2, I4, and I5), suggesting that ampicillin binding hindered the solvent explosion as supporting the experimental results in Section 3.1.1. The perturbation increase in accessible surface area of PECs due to addition of HA was evident, leading to increased SASA values supporting the results in Figure 1. The I2 formulation unloaded and produced with the highest HA ratio (12% HA added formulation) had the highest swelling ındex versus time. This observation suggests that higher quantities of HA enhance PECs' hydrodynamics, resulting in greater solvent exposure. Consequently, this reduces drug binding by diminishing its hydrophobic behavior in the aqueous solution.

4. CONCLUSIONS

The simulation data revealed the formation of PECs drug delivery systems loaded with ampicillin through a combination of hydrophobic and hydrophilic interactions, rendering them suitable for targeted drug delivery to treat periodontitis. It became evident that the interaction between the drug and

https://doi.org/10.1021/acsomega.3c08076
ACS Omega 2024, 9, 19805−19815

PECs was influenced by the presence of HA. This influence was discernible in the structural dynamics and transport properties of the simulated system. Notably, the variation in the amount of HA played a pivotal role in modulating the release of the drug from the delivery system.

Assessing the dynamic and transportation properties of these simulation systems proved instrumental in determining the drug-binding capacity and the flexibility of drug release from the carrier, which consisted of PECs, chitosan, and HA. Notably, the addition of HA was observed to enhance these properties, improving drug release.

Furthermore, the examination of different energy components emerged as a critical factor in designing an effective drug delivery system. It was established that the interaction between ampicillin and PECs, especially in a larger quantity of HA, resulted in a more efficient drug delivery mechanism compared to scenarios with lower HA levels.

Overall, this model study sets the stage for further exploration of various combinations of chitosan and HA, whether natural or synthetic, in conjunction with ampicillin, with the aim of developing a more efficient targeted drug delivery system for the treatment of periodontitis.

■ ASSOCIATED CONTENT

Data Availability Statement

Data will be made available on request.

■ AUTHOR INFORMATION

Corresponding Author

Khair Bux − *Faculty of Life Sciences, Department of Biosciences, Shaheed Zulfikar Ali Bhutto Institute of Science and Technology (SZABIST), Karachi 75600, Pakistan;* orcid.org/0000-0003-2440-0116; Email: khair.bux@szabist.edu.pk, ali.compchemist@gmail.com

Authors

Sema Arısoy − *Faculty of Pharmacy, Department of Pharmaceutical Technology, Selcuk University, Konya 42250, Turkey*

Ralf Herwig − *Laboratories PD Dr. R. Herwig, 80337 Munich, Germany; Heimerer-College, Pristina 10000, Kosovo*

Emine Şalva − *Faculty of Pharmacy, Department of Pharmaceutical Biotechnology, Inonu University, Malatya 44210, Turkey*

Complete contact information is available at: https://pubs.acs.org/10.1021/acsomega.3c08076

Author Contributions

S.A.: Conceptualization, Experimental design, Supervision, Investigation, Writing—review and editing. K.B.: Conceptualization, Experimental design, Supervision, Investigation, Writing—review and editing. R.H.: Supervision, E.S.: Supervision.

Notes

The authors declare no competing financial interest.

■ ACKNOWLEDGMENTS

This research did not receive any specific grant from funding agencies in the public, commercial, or not-for-profit sectors.

■ REFERENCES

(1) Listgarten, M. A. Pathogenesis of periodontitis. *J. Clin. Periodontol.* **1986**, *13* (5), 418−425.

(2) H.r, R.; et al. Local drug delivery systems in the management of periodontitis: A scientific review. *J. Control. Release* **2019**, *307*, 393−409.

(3) Joshi, D.; et al. Advanced drug delivery approaches against periodontitis. *Drug Delivery* **2016**, *23* (2), 363−377.

(4) Piras, A. M.; et al. Chitosan Nanoparticles for the Linear Release of Model Cationic Peptide. *Pharm. Res.* **2015**, *32* (7), 2259−2265.

(5) Kilicarslan, M.; et al. Preparation and evaluation of clindamycin phosphate loaded chitosan/alginate polyelectrolyte complex film as mucoadhesive drug delivery system for periodontal therapy. *European Journal of Pharmaceutical Sciences* **2018**, *123*, 441−451.

(6) Wei, Y.; et al. Local drug delivery systems as therapeutic strategies against periodontitis: A systematic review. *J. Controlled Release* **2021**, *333*, 269−282.

(7) Noel, S. P.; et al. Chitosan Films: A Potential Local Drug Delivery System for Antibiotics. *Clinical Orthopaedics and Related Research* **2008**, *466* (6), 1377−1382.

(8) Shu, X. Z.; Zhu, K. J. The influence of multivalent phosphate structure on the properties of ionically cross-linked chitosan films for controlled drug release. *Eur. J. Pharm. Biopharm.* **2002**, *54* (2), 235−243.

(9) Rezaei, F. S.; et al. Chitosan films and scaffolds for regenerative medicine applications: A review. *Carbohydr. Polym.* **2021**, *273*, No. 118631.

(10) Nguyen, N.T.-P.; et al. The effect of oxidation degree and volume ratio of components on properties and applications of in situ cross-linking hydrogels based on chitosan and hyaluronic acid. *Materials Science and Engineering: C* **2019**, *103*, 109670.

(11) Miranda, D. G.; et al. A chitosan-hyaluronic acid hydrogel scaffold for periodontal tissue engineering. *Journal of Biomedical Materials Research Part B: Applied Biomaterials* **2016**, *104* (8), 1691−1702.

(12) Akıncıbay, H.; Şenel, S.; Yetkin ay, Z. Application of chitosan gel in the treatment of chronic periodontitis. *J. Biomed. Mater. Res. B: Appl. Biomater.* **2007**, *80* (2), 290−296.

(13) Khajuria, D. K.; et al. Development and evaluation of novel biodegradable chitosan based metformin intrapocket dental film for the management of periodontitis and alveolar bone loss in a rat model. *Archives of Oral Biology* **2018**, *85*, 120−129.

(14) Ahmadi, H.; Ebrahimi, A.; Ahmadi, F. Antibiotic therapy in dentistry. *Int. J. Dent.* **2021**, *2021*, No. 6667624, DOI: 10.1155/2021/6667624.

(15) Schkarpetkin, D.; et al. Development of novel electrospun dual-drug fiber mats loaded with a combination of ampicillin and metronidazole. *Dental Materials* **2016**, *32* (8), 951−960.

(16) Bunker, A.; Róg, T. Mechanistic understanding from molecular dynamics simulation in pharmaceutical research 1: Drug delivery. *Frontiers in Molecular Biosciences* **2020**, *7*, No. 604770.

(17) Bernal-ballen, A.; Lopez-garcia, J.-A.; Ozaltin, K. (PVA/Chitosan/Fucoidan)-Ampicillin: A Bioartificial Polymeric Material with Combined Properties in Cell Regeneration and Potential Antibacterial Features. *Polymers* **2019**, *11* (8), 1325.

(18) Shen, J.-W.; et al. Molecular dynamics study on the mechanism of polynucleotide encapsulation by chitosan. *Sci. Rep.* **2017**, *7* (1), 5050.

(19) Wang, J.; et al. Antechamber: an accessory software package for molecular mechanical calculations. *J. Am. Chem. Soc.* **2001**, *222* (1), 2001.

(20) Van der spoel, D.; et al. GROMACS: fast, flexible, and free. *Journal of computational chemistry* **2005**, *26* (16), 1701−1718.

(21) Jorgensen, W. L.; et al. Comparison of simple potential functions for simulating liquid water. *J. Chem. Phys.* **1983**, *79* (2), 926−935.

(22) Hess, B.; et al. LINCS: A linear constraint solver for molecular simulations. *Journal of computational chemistry* **1997**, *18* (12), 1463−1472.

(23) Darden, T.; York, D.; Pedersen, L. Particle mesh Ewald: An N·log (N) method for Ewald sums in large systems. *J. Chem. Phys.* **1993**, *98* (12), 10089−10092.
(24) James, T. C. Calculations of collision narrowing of the quadrupole lines in molecular hydrogen. *JOSA* **1969**, *59* (12), 1602−1606.
(25) Bussi, G.; Donadio, D.; Parrinello, M. Canonical sampling through velocity rescaling. *J. Chem. Phys.* **2007**, *126* (1), No. 014101, DOI: 10.1063/1.2408420.
(26) Koo, G. N.; et al. Molecular dynamics study on the binding of S-and R-ofloxacin to [d (ATAGCGCTAT)] 2 oligonucleotide: effects of protonation states. *Bull. Korean Chem. Soc.* **2008**, *29* (11), 2103.
(27) Fletcher, R.; Powell, M. J. A rapidly convergent descent method for minimization. *computer journal* **1963**, *6* (2), 163−168.
(28) Humphrey, W.; Dalke, A.; Schulten, K. VMD: visual molecular dynamics. *J. Mol. Graphics* **1996**, *14* (1), 33−38.
(29) Ilyas, A.; Poddar, N. K.; Borkotoky, S. Insights into the dynamic interactions of RNase a and osmolytes through computational approaches. *J. Biomol. Struct. Dyn.* **2023**, 1−9.
(30) Zeeshan, R.; et al. Hydroxypropylmethyl cellulose (HPMC) crosslinked chitosan (CH) based scaffolds containing bioactive glass (BG) and zinc oxide (ZnO) for alveolar bone repair. *Carbohydr. Polym.* **2018**, *193*, 9−18.
(31) Ali, H. U.; et al. HPMC crosslinked chitosan/hydroxyapatite scaffolds containing Lemongrass oil for potential bone tissue engineering applications. *Arabian Journal of Chemistry* **2022**, *15* (7), No. 103850.
(32) Combes, F. C.; Canizares, O. Sulfanilamide and Allied Compounds: Their Value and Limitations in Dermatology. *Archives of Dermatology and Syphilology* **1941**, *44* (2), 236−247.
(33) Arisoy, S.; et al. Development of ACE2 loaded decoy liposomes and their effect on SARS-CoV-2 for Covid-19 treatment. *Pharm. Dev. Technol.* **2022**, *27* (3), 290−300.
(34) Prakash, C.; et al. Skin surface pH in acne vulgaris: insights from an observational study and review of the literature. *J. Clin. Aesthet. Dermatol.* **2017**, *10* (7), 33−39.
(35) Şalva, E.; et al. Investigation of therapeutic effects in the wound healing of chitosan/pGM-CSF complexes. *Braz. J. Pharm. Sci.* **2022**, *58*, No. e19668.
(36) Khaled, S. A.; et al. Extrusion 3D printing of paracetamol tablets from a single formulation with tunable release profiles through control of tablet geometry. *Aaps Pharmscitech* **2018**, *19* (8), 3403−3413.
(37) Xu, Y.; et al. Nanoparticles based on chitosan hydrochloride/hyaluronic acid/PEG containing curcumin: In vitro evaluation and pharmacokinetics in rats. *Int. J. Biol. Macromol.* **2017**, *102*, 1083−1091.
(38) Nath, S. D.; et al. Chitosan−hyaluronic acid polyelectrolyte complex scaffold crosslinked with genipin for immobilization and controlled release of BMP-2. *Carbohydr. Polym.* **2015**, *115*, 160−169.
(39) Duran, S.; Anwar, J.; Moin, S. T. Interaction of gentamicin and gentamicin-AOT with poly-(lactide-co-glycolate) in a drug delivery system - density functional theory calculations and molecular dynamics simulation. *Biophys. Chem.* **2023**, *294*, No. 106958.
(40) Yarce, C. J.; Echeverri, J. D.; Salamanca, C. H. Effect of the Surface Hydrophobicity Degree on the In Vitro Release of Polar and Non-Polar Drugs from Polyelectrolyte Matrix Tablets. *Polymers* **2018**, *10* (12), 1313.
(41) Haroosh, H. J.; et al. Improvement of drug release and compatibility between hydrophilic drugs and hydrophobic nanofibrous composites. *Materials* **2021**, *14* (18), 5344.

https://doi.org/10.1021/acsomega.3c08076
ACS Omega 2024, 9, 19805−19815